Alterations of Slow and Fast Rod ERG Signals in Patients with Molecularly Confirmed Stargardt Disease Type 1

Hendrik P. N. Scholl,[1,2] *Dorothea Besch,*[1] *Reinhard Vonthein,*[3] *Bernhard H. F. Weber,*[4] *and Eckart Apfelstedt-Sylla*[1]

Purpose. To investigate the slow and fast rod signals of the scotopic 15-Hz flicker ERG in patients with molecularly confirmed Stargardt disease type I (STGD1). There is evidence that these slow and the fast rod ERG signals can be attributed to the rod bipolar–AII cell pathway and the rod–cone coupling pathway, respectively.

Methods. Twenty-seven patients with STGD1 with mutations in both alleles of the *ABCA4* gene were included. Scotopic ERG response amplitudes and phases to flicker intensities ranging from −3.37 to −0.57 log scotopic troland · sec (log scot td · sec) were measured at a flicker frequency of 15 Hz. In addition, scotopic standard ERGs were obtained. Twenty-two normal subjects served as controls.

Results. The amplitudes of both the slow and fast rod ERG signals were significantly reduced in the STGD1 group. The phases of the slow rod signals lagged significantly, whereas those of the fast rod signals did not. The standard scotopic ERG did not reveal significant alterations.

Conclusions. The results provide evidence that a defective ABCA4 transporter can functionally affect both the rod bipolar–AII cell pathway and the rod–cone coupling pathway. In STGD1, the scotopic 15-Hz flicker ERG may reveal subtle abnormalities at different sites within the rod system that remain undetected by standard ERG techniques. (*Invest Ophthalmol Vis Sci.* 2002;43:1248–1256)

The protein ABCA4 (formerly ABCR) is a rod and cone cell-specific member of the ATP-binding cassette family of transporters. It was independently identified as an abundant 250-kDa photoreceptor outer segment membrane protein[1–4] and as the protein product of a retina-specific gene, *ABCA4*, that is mutated in chromosome 1–linked autosomal recessive Stargardt macular dystrophy-fundus flavimaculatus (STGD1; Online Mendelian Inheritance in Man [OMIM]: 248200; provided by the National Center for Biotechnology, Bethesda, MD, and available at http://www3.ncbi.nlm.nih.gov/omim/).[5] Mutations in *ABCA4* responsible for STGD1 are found throughout the protein-coding region.[5–10] The clinical disease was first described by the German ophthalmologist Karl Stargardt as a unique macular dystrophy characterized by visual loss in the first two decades of life in combination with an atrophic lesion of the macula.[11] Franceschetti later used the term fundus flavimaculatus to denote a retinal dystrophy characterized by yellow flecks found in the distal retina at the posterior pole of the eye.[12] Intrafamilial coexistence of the two different funduscopic patterns has been observed frequently,[13] and linkage analysis has recently revealed that Stargardt macular dystrophy and fundus flavimaculatus genetically represent a single disorder.[14]

Clinically, STGD1 compromises mainly macular function,[15] and recently it has been shown that *ABCA4* is expressed both in foveal and peripheral cones.[16] In accordance with *ABCA4* expression in cones, we showed recently that patients with STGD1 can exhibit substantial amplitude and phase alterations of long (L)- and middle (M)-wavelength cone driven photopic ERGs with a large interindividual variability.[17] However, in previous studies ABCA4 appeared to be a protein exclusively confined to rod outer segments,[5] and studies in *ABCA4* knockout mice point to an important role of the rod system in the pathophysiology of the disease.[18] To better understand the ABCA4-mediated mechanism in human disease, the investigation of rod function in patients carrying *ABCA4* mutations is advisable. ERG surveys on rod function involving standard techniques have been equivocal.[13,19–26] Moreover, in none of these studies have the patients been genotyped.

Our preliminary observations have suggested that subtle deterioration within the rod system that is not visible with the standard rod ERG may be detected by means of the scotopic 15-Hz flicker ERG in patients with molecularly confirmed STGD1.[27] Moreover, there is plenty of evidence that the slow and fast rod signals derived from the scotopic 15-Hz flicker ERG reflect electrophysiological activity driven by two different rod circuitries: the rod bipolar–AII cell pathway and the rod–cone coupling pathway, respectively.[28–30] Histologic studies of the human retina in STGD1 have reported Müller cell hypertrophy and lipofuscin granules in the inner segments.[31] These changes may well alter postreceptoral rod function. Therefore, the purpose of the present study was to extend ERG testing in STGD1 toward a protocol capable of testing function of different postreceptoral rod circuitries.

Although it is undisputed that typical STGD1 is an autosomal recessive disorder in most affected families, standard techniques identify mutations in only approximately 60% of *ABCA4* alleles.[6,7,10] Thus, it is mandatory for a study attempting to correlate retinal function with the STGD1 genotype to be confined to those patients in whom both mutant alleles have been identified. We therefore exclusively included in our study patients with STGD1 who had mutations in both alleles of the *ABCA4* gene.[10]

From the [1]Department of Pathophysiology of Vision and Neuroophthalmology, University Eye Hospital Tübingen, Tübingen, Germany; the [2]Institute of Ophthalmology, Moorfields Eye Hospital, London, United Kingdom; the [3]Department of Medical Biometry, University of Tübingen, Tübingen, Germany; and the [4]Institute of Human Genetics, Biocenter, University of Würzburg, Würzburg, Germany.

Supported by *f*ortüne-Grant 707-0-1, Tübingen, Germany (HPNS); Deutsche Forschungsgemeinschaft We 1259/10-1 (BHFW), and Ap 57/3-1 (EA-S).

Submitted for publication May 29, 2001; revised October 15, 2001; accepted November 19, 2001.

Commercial relationships policy: N.

The publication costs of this article were defrayed in part by page charge payment. This article must therefore be marked "*advertisement*" in accordance with 18 U.S.C. §1734 solely to indicate this fact.

Corresponding author: Eckart Apfelstedt-Sylla, Katharinenhospital, Augenklinik, Kriegsbergstrasse 60, D-70174 Stuttgart, Germany; apfelstedt-sylla@katharinenhospital.de.

Investigative Ophthalmology & Visual Science, April 2002, Vol. 43, No. 4

METHODS

Patients with STGD1 and Normal Subjects

Twenty-seven patients were included in the study. A detailed history (including family history) was obtained and a comprehensive ophthalmic examination (including visual acuity, which was measured on a quasilogarithmic ordinal scale; for use in regression models it was ranked 1–10 and treated as quasicontinuous) was performed. Fundus appearances were assessed by slit lamp biomicroscopy and color fundus photographs. In the literature, there is no uniform classification of the fundus changes in STGD1. As previously reported,[17] we staged the central fundus changes from mild (normal to diffuse foveal reflex, subtle pigment mottling of the macular retinal pigment epithelium [RPE], tapetal sheen or beaten-bronze reflex), to moderate (pronounced hyper- and hypopigmentation of the macular RPE, bull's-eye atrophy), to severe (widespread confluent areas of RPE and/or choroidal atrophy). In addition, the existence and distribution of the typical white-yellow flecks at the level of the RPE were staged: (−) no flecks; (+) flecks confined to the posterior pole (i.e., within the vascular arcades); and (++) peripheral flecks extending beyond the vascular arcades. The fundus alterations were very similar in the two eyes in each patient. For statistical analysis, we evaluated the fundus features (distribution of flecks) of only one eye (which was randomly chosen).

Twenty-two normal subjects served as the control. Detailed ERG data on this group of normal subjects have been published previously.[27] Both the 15-Hz scotopic flicker ERG and the scotopic standard ERG were recorded from the same set of normal subjects.

Informed consent was obtained from all subjects after explanation of the purpose and possible consequences of the study. This study was conducted in accordance with the tenets of the Declaration of Helsinki and with the approval of our institutional ethics committee on human experimentation.

Mutation Analysis in the *ABCA4* Gene

The 27 patients were selected from a large study group, based on their harboring disease-associated mutations on both *ABCA4* alleles.[10] Details on the mutation analysis are fully described elsewhere.[10]

ERG Stimulation, Recording, and Procedure

The apparatus, the stimulation, and the procedure of the ERG measurements have been reported.[27] Briefly, we used a Ganzfeld stimulator (LKC Technologies, Inc., Gaithersburg, MD) and data acquisition system (Universal Testing and Analysis System-Electrophysiology 2000 [UTAS-E 2000]; LKC Technologies, Inc.). Stimulus and recording conditions were in accordance with the International Society for Clinical Electrophysiology of Vision (ISCEV) standard.[32] The subjects, positioned with the aid of a headrest, viewed into the center of a Ganzfeld bowl. The bowl was homogeneously illuminated by white flashes repeated at a frequency of 15 Hz produced by a xenon discharge lamp (flash duration ~10 μs; correlated color temperature ~6000 K; see Table 1 [2.4.4] in Ref. 33). The flicker yielded by this device was full field. To avoid stray light, we masked all sites of light leakage by black tape. In addition, the subjects were surrounded by a black curtain so that accidental light or stray light (e.g., arising from the computer monitor) had no influence on the Ganzfeld illumination and the ERG recording. Each flash was triggered by the testing system's computer (UTAS-E 2000; LKC Technologies, Inc.), which was also used to store and analyze the ERG recordings. Maximal intensity was 1.43 log scotopic troland · sec (log scot td · sec). To attenuate the flash, neutral density (ND) filters (Wratten; Eastman Kodak, Rochester, NY) mounted in a filter wheel were inserted. The maximum attenuation was 4.8 log units ND and the step size was 0.2 log units ND. Thus, the minimum stimulus intensity was at approximately −3.37 log scot td · sec. We continued the measurements up to a retinal illuminance of −0.57 log scot td · sec, which is well below the cone threshold in the Ganzfeld ERG (approximately 0.75 log scot td · sec[34]).

Each subject was dark adapted for 30 minutes. In the normal subjects, one eye was dilated with a mydriatic agent (0.5% tropicamide), and in the patients, tropicamide (0.5%) and phenylephrine (5%) were used. Pupil diameters were determined before ERG recordings. There was no difference in pupil diameter between the two subject groups. Dawson, Trick, Litzkow (DTL) fiber electrodes were positioned on the conjunctiva directly beneath the cornea and attached at the nasal and lateral canthus. Reference electrodes (Ag-AgCl) were placed over both temporal bones, and a ground electrode was placed on the forehead. The ERG responses to the periodic flashes were recorded and stored by means of the testing system's computer. To avoid the effects of the rapid changes of gain control mechanisms in the rod system that accompany the onset of flickering lights, we discarded the responses to the flashes presented during the first 5 seconds. The signals were bandpass filtered (1–70 Hz) and averaged 50 to 100 times online. The noise level was determined by recording an ERG signal with the xenon discharge lamp covered by black cardboard (similar to a published procedure[35]). In addition, we performed a scotopic ERG according to the ISCEV standard,[32] by using the same setup. For the rod response (b-wave), the patients and normal subjects were dark adapted for at least 30 minutes before recording began. The stimulus was a dim white flash of −0.97 log scot td · sec (2.4 log units below the standard white flash). For the maximal combined response (a-wave and b-wave), we then used a standard white flash of 1.43 log scot td · sec.

Data Analysis

To determine the periodicity of the ERG responses, we computed a fast Fourier transform (FFT) on the sampled data.[36,37] As a result, we found that all responses were dominated by the fundamental component.[27] Therefore, we identified the ERG response amplitude and phase as the amplitude and phase of this fundamental component. In a previous study in normal subjects, we found that the flicker null (and the large phase shift of approximately 180°) occurs between intensities of −1.77 and −1.37 log scot td · sec.[27] Therefore, the ERG signals at flicker intensities between −3.37 and −1.97 log scot td · sec (eight intensity levels) were considered to be dominated by the slow rod ERG signals and ERG signals between −1.17 and −0.57 log scot td · sec (four intensity levels) by the fast rod ERG signals.

Statistical Analysis

Data were analyzed by computer (JMP software, ver. 4.0.2; SAS Institute, Inc., Cary, NC). Results with $P < 0.05$ were considered statistically significant. For descriptive statistics (such as the median and the percentiles for the standard ERG measures), we considered both the right and left eyes of each patient. To estimate how many patients with STGD1 exhibited abnormal ERG signals of the two rod ERG pathways, we summed up the ERG amplitudes obtained at flicker intensities between −3.37 and −1.97 log scot td · sec (for the slow rod ERG pathway) and those obtained at flicker intensities between −1.17 and −0.57 log scot td · sec (for the fast rod ERG pathway) and compared this measure with the normal 5th percentile.

For hypothesis testing, the amplitudes and implicit times of the slow and fast rod ERG signals of the patients with STGD1 were compared with those of normal subjects by a multivariate repeated-measures analysis of variance (MANOVA) with an "eye" factor, because the data from patients in the STGD1 group were from two eyes that are not independent.[38] Thus, we tested the difference between the multivariate means of the normal subjects' and the patients' eyes with degrees of freedom equal to the number of persons and countered the larger variation in the patients' ERG responses amplitude and phases by effectively averaging over the two eyes of each patient. In a recent study on patients with X-linked congenital stationary night blindness carrying mutations in the *NYX* gene, the same statistical approach was used.[39]

To evaluate interocular differences in the patients' group we calculated the median of the differences between the two eyes of each

patient at every flicker intensity level for both the logarithm of the ERG amplitude and the ERG response phase. To correlate the intraindividual interocular differences with the visual acuity, we calculated the difference of the amplitudes and phases of the better eye (in visual acuity) minus those of the worse eye. For every intensity level, we then calculated the mean ± SE of all the patients' data and tested the hypothesis that this difference is zero.

For the standard ERG parameters, a similar analysis of variance (ANOVA) with the patient as a random factor was used. We furthermore performed a multivariate repeated-measures analysis of covariance (MANCOVA) to assess the effect of explanatory variables such as age, age-adjusted disease duration, visual acuity, and distribution of flecks on both the scotopic 15-Hz flicker ERG and the standard rod ERG. How standard ERG and slow and fast rod ERG measures coincide was described by canonical correlation (i.e., the maximal correlation between linear combinations).

Results

Group Characteristics

The ages of the patients with STGD1 (range, 13–55 years; median, 32) did not differ significantly ($P = 0.95$, unpaired *t*-test) from those of the 22 normal subjects (range, 19–58 years; median, 29.5). Subject groups did not differ in their proportion of male-to-female subjects ($P = 0.39$, two-tailed Fisher exact test). Clinical data on the patients with STGD1 are shown in Table 1.

Mutation Analysis in the *ABCA4* Gene

In the 27 patients with STGD1 included in the study, disease-causing mutations were identified in all 54 *ABCA4* alleles[10] (Table 1). Eleven patients were found to carry missense mutations in both alleles, whereas 11 patients had a missense mutation in one and a second mutation in the other allele, which is expected to result in a truncated protein (i.e., two nonsense, two frameshift, seven splice mutations). Five patients (numbers 15, 18, 19, 26, 27) were shown to have a 2588G→C splice mutation in one allele in combination with a nonsense (Q1412X or Q1750X) or a splice (IVS35+2T→A) mutation in the other allele (Table 1).

Amplitudes of the Slow and Fast Rod ERG Signals

Figure 1 displays the original ERG signals to visual stimulation of the 15-Hz flicker at scotopic conditions in a normal subject (left) and a patient with STGD1 (patient 15; right). In the normal subject, the ERG signal increased slightly with increasing flicker intensity from −3.37 to −2.97 log scot td · sec and then decreased thereafter. There was a gradual increase (advance) in the response phase with increasing flicker intensity. At flicker intensities between −2.17 and −1.77 log scot td · sec, there was a minimum in ERG response. To higher flicker intensities (from −1.37 to −0.97 log scot td · sec), the ERG signal rapidly increased again in amplitude and was considerably phase advanced. In patient 15, the features described for the normal subject were similar; however, the patient displayed reduced ERG signals for both the lower and the higher flicker intensity ranges, even though the patient's amplitudes were considerably above the median of those of the patients with STGD1 as a group.

The ERG signals were Fourier analyzed, and the amplitude and phase of the fundamental component were determined. In Table 1, we provide a surrogate of the signal reduction within

Table 1. Characteristics of the 27 patients with STGD1

Patient	Sex	Age	Onset	VA (OD)	VA (OS)	CFC	DF	Mut(1)	Mut(2)	Slow Rod ERG	Fast Rod ERG
1	M	32	9	1/50	20/400	Severe	++	Q1412X	R2077W	19.2	12.1
2	M	49	17	20/200	20/200	Severe	+	768G→T	G1961E	56.1	23.8
3	M	46	30	20/40	20/200	Mild	+	E471K	G1961E	31.7	29.0
4*	M	27	19	20/32	20/100	Moderate	+	2588G→C	E1885K	35.0	45.1
5*	M	31	18	20/400	20/400	Severe	++	2588G→C	E1885K	36.1	39.1
6*	F	29	12	20/200	20/200	Moderate	++	2588G→C	E1885K	23.4	8.1
7	F	23	18	20/400	20/400	Mild	++	E1399K	G1977S	103.5	39.3
8	M	28	17	20/200	20/200	Mild	++	R1898H	G1975R	44.4	19.5
9	M	39	29	20/100	20/200	Moderate	+	G607R	G1961E	45.8	20.7
10	F	23	17	20/200	20/200	Mild	−	P68L	S1689P	80.2	25.9
11	F	33	30	20/50	20/50	Mild	−	E1399K	G1961E	49.8	62.0
12	M	50	42	20/400	20/64	Severe	++	2588G→C	L541P/A1038V	53.8	30.2
13	M	36	25	20/40	20/32	Moderate	++	296insA	A1038V	88.2	40.0
14	F	55	16	HM	HM	Severe	++	Q635K	IVS40+5G→A	11.7	11.2
15	F	27	25	20/100	20/50	Moderate	+	2588G→C	Q1412X	65.8	71.5
16	F	45	14	1/50	1/35	Severe	++	L541P/A1038V	S1063P	16.4	16.6
17	M	40	23	20/100	20/200	Moderate	+	296insA	G1961E	46.1	58.3
18**	M	35	15	20/400	20/400	Moderate	+	2588G→C	Q1750X	14.1	12.9
19**	M	43	14	HM	HM	Severe	++	2588G→C	Q1750X	17.4	8.6
20	F	32	8	20/200	20/200	Severe	+	G1961E	G1961E	66.2	79.0
21	F	23	12	20/400	20/400	Mild	−	R212C	T9591	24.6	25.3
22	F	29	9	20/200	20/200	Moderate	+	L541P/A1038V	G1961E	72.3	31.8
23	M	20	9	20/400	20/400	Moderate	++	L541P/A1038V	IVS40+5G→A	64.7	42.2
24	F	39	23	20/400	20/50	Moderate	−	W663X	G1961E	92.6	68.8
25	F	41	36	20/200	20/64	Severe	+	F1440V	G1748R	97.2	52.7
26***	M	13	10	20/100	20/200	Moderate	−	R572Q/2588G→C	IVS35+2T→A	59.2	33.5
27***	M	16	15	20/200	20/200	Moderate	+	R572Q/2588G→C	IVS35+2T→A	31.1	22.9

Age at examination (y), gender, age of onset (y), visual acuity (VA), central fundus changes (CFC), and existence and distribution of the typical white-yellow flecks (DF) are shown. In addition, the molecular genetic findings in the *ABCA4* gene are specified (Mut 1 and 2). The last two columns provide the percentage of ERG amplitude for the slow and fast rod ERG signals (average of the right and left eye) compared with the mean of the normal subjects for the individual patients (for calculation procedure see Ref. 27).

* Siblings. HM, visual acuity decreased to hand motions.

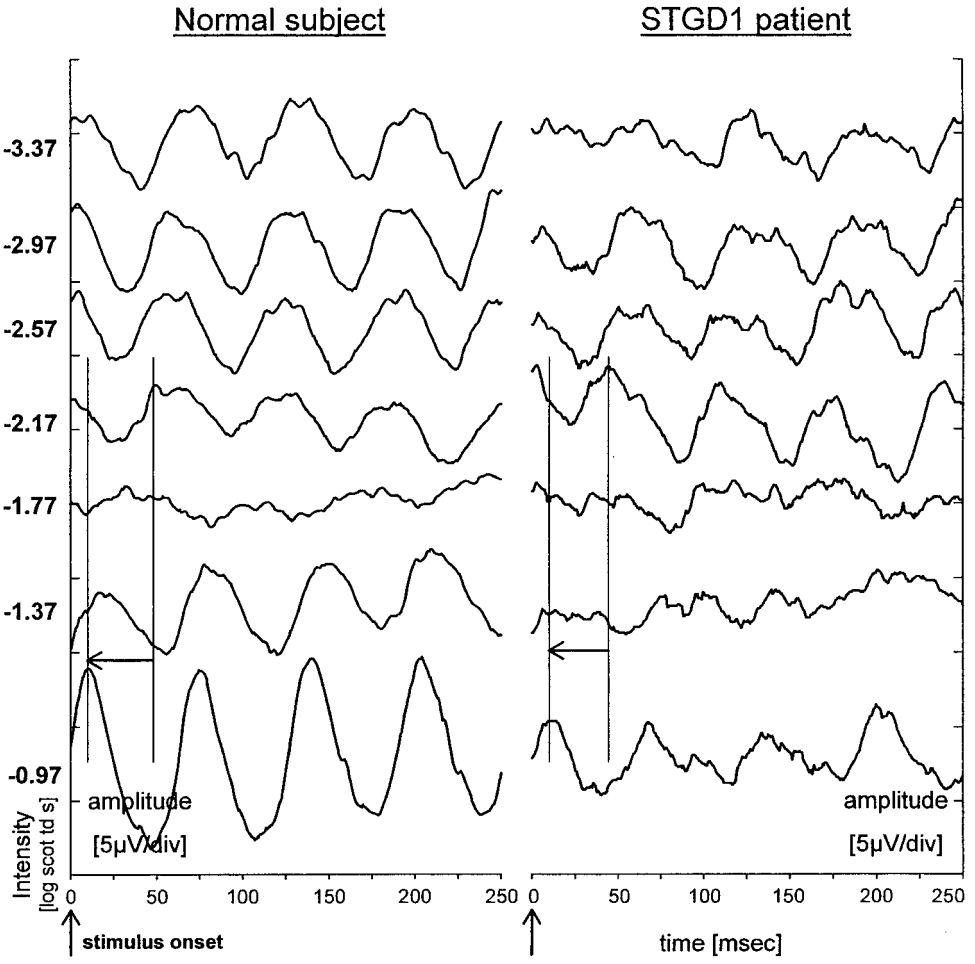

FIGURE 1. Original tracings of the rod ERG responses to 15-Hz flicker stimulation obtained from a normal subject (*left*) and a patient with STGD1 (patient 15, *right*). Shown is 250 ms of the ERG signal. The origin of the *x*-axis indicates stimulus onset. On the *y*-axis, the flicker intensity at which the ERG response was obtained is shown. Step size is 0.4 log units ND attenuation of the maximal intensity, beginning with the lowest intensity of −3.37 log scot td · sec (*top*). One division indicates 5 μV. In the normal subject, two features were observed: The amplitude increased somewhat with increasing flicker intensity and then decreased to a minimum at −1.77 log scot td · sec with a rapid increase of the ERG response amplitude thereafter. With increasing flicker intensity, there was a shift of the timing of the ERG signal toward larger phases (corresponding to shorter implicit times, *arrow*). The features in the patients with STGD1 were similar, but there was a considerable amplitude loss for both the lower and higher flicker intensities.

the two rod ERG pathways for each patient separately (for calculation procedure, see Ref. 27). The data in the table allow a qualitative estimation of the severity of rod dysfunction in view of the mutation pairings and the other clinical parameters, such as age of onset. For instance, patient 20, who was homozygous for the G1961E mutation, exhibited the earliest onset (8 years of age) but relatively mild reductions of both the slow and fast rod ERG signals. This is also true of patients 22 and 23 (onset at 9 years). Patient 1, however, who also showed an early onset (9 years), carrying the mutations Q1412X and R2077W, exhibited severely reduced amplitudes of the slow and fast rod ERG signals. Patient 13, carrying the mutations 296insA and G1961E, exhibited the latest onset (42 years). The amplitude reductions for both the slow and fast rod ERG signals, however, were near the median of the patient study group.

In Figure 2, the noise level and the median, the 5th and 95th percentiles of both the normal subjects and the patients with STGD1 are displayed. As a group, the patients exhibited considerably reduced amplitudes for both the slow and the fast rod ERG signals. However, there was an overlap between the data sets of patients and normal subjects. Considering the summed ERG amplitudes for the slow and fast rod signals for each eye of each patient, 19 and 37 of 54 eyes, respectively, were below the normal 5th percentile.

To explore whether the two subject groups showed statistically significant differences, the amplitudes of the slow (eight intensity levels) and the fast (four intensity levels) rod ERG signals were statistically analyzed using a repeated-measures MANOVA with the factors "disease" and "eye nested under subject and disease." Because residuals of amplitudes for both rod ERG pathways do not have a normal distribution, we converted amplitudes into their logarithms, which had normal distributed residuals. For the two rod ERG pathways, the

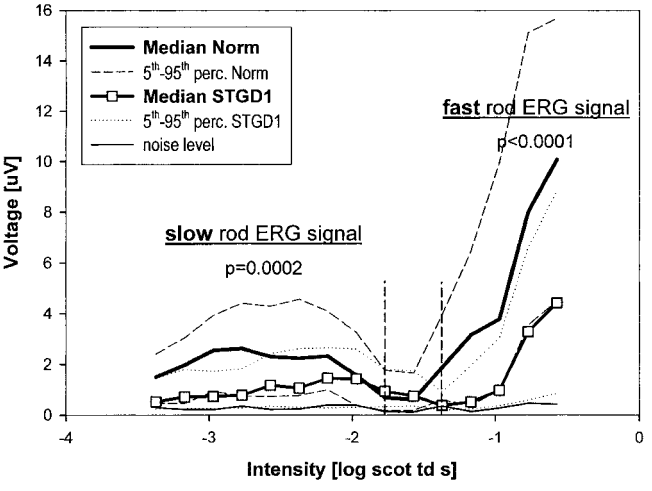

FIGURE 2. Rod ERG amplitudes to 15-Hz flicker stimulation with increasing flicker intensity in the normal subjects and the patients with STGD1. In the patients with STGD1, considerable amplitude decreases were observed in both the slow and the fast rod ERG signals. The probabilities indicate the results obtained by MANOVA of the amplitude data.

MANOVA revealed significantly lower amplitudes in the patients with STGD1 for both the slow (F test, exact F = 16; $P = 0.0002$) and the fast (F = 31; $P < 0.0001$) rod ERG signals. The intraindividual interocular differences were considerably low (median for the slow rod ERG signals between 0.09 and 0.13 μV; for the fast rod ERG signals between 0.07 and 0.15 μV) indicating that the amplitude data were very similar in the two eyes in individual patients. Probabilities for testing the hypothesis that eyes with better visual acuity exhibited larger amplitudes ranged between 0.20 and 0.80 for the slow rod ERG signals and between 0.30 and 0.80 for the fast rod ERG signals, indicating that there was no significant correlation of intraindividual differences.

To test for the relationship between the clinical parameters (age, age-adjusted disease duration, visual acuity, distribution of flecks; see Table 1) and the amplitudes of the slow rod ERG pathway, a repeated-measures MANCOVA was used. The MANCOVA revealed that all these clinical parameters together influenced the amplitude data significantly (F = 4.8; $P = 0.0007$). However, just one single regressor had a probability just less than 0.05—namely, visual acuity (F = 4.7; $P = 0.04$).

For the fast rod ERG pathway, a similar MANCOVA revealed that the combination of age, age-adjusted disease duration, visual acuity, and the distribution of flecks influenced the amplitude data significantly (F = 4.6; $P = 0.0009$). However, no single regressor influenced these ERG amplitudes significantly.

Phases of the Slow and Fast Rod ERG Signals

Consistent with destructive interference between the slow and fast rod ERG signals being the cause of the amplitude minimum shown in Figures 1 and 2, the phase of the ERG responses abruptly increased by approximately 180° (corresponding to a half cycle) as the amplitude minimum was crossed (Fig. 3). For the phases of the slow rod ERG signal, a considerable decrease (corresponding to a slowing of the signal, provided that a time delay difference is the cause of the phase difference) was observed in the patients with STGD1. This was true of each of the eight phases obtained at the lower flicker intensities (Fig. 3). Of the phases obtained at the highest flicker intensities corresponding to the fast rod ERG signals, only the ERG response phase obtained at −1.17 log scot td · sec showed a noticeable reduction, whereas the phases obtained at flicker intensities between −0.97 and −0.57 log scot td · sec were rather similar to those of the normal subjects (Fig. 3).

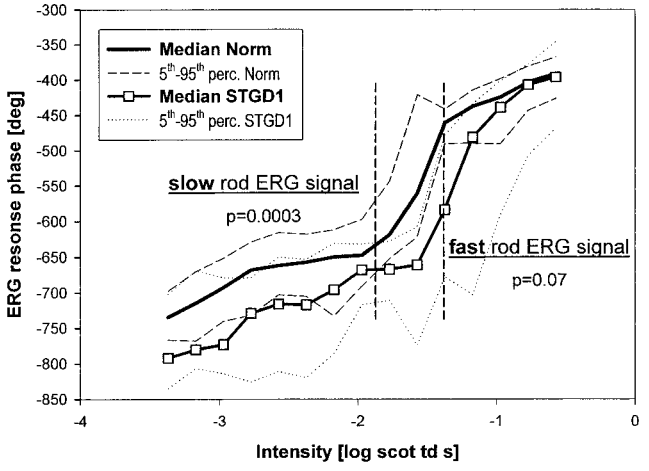

FIGURE 3. Rod ERG phases to 15-Hz flicker stimulation with increasing flicker intensity in the normal subjects and the patients with STGD1. In slow rod ERG signals, the patients with STGD1 showed considerably reduced phases, whereas the phases were rather similar between the two subject groups in fast rod ERG signals. The probabilities indicate the results obtained by the MANOVA of the phase data.

As performed for the amplitude data, the phases of the slow and the fast rod ERG signals were statistically analyzed using a repeated-measures MANOVA with factors "disease" and "eye nested under subject and disease." The MANOVA revealed that the phases of the slow rod ERG signals lagged significantly in the patients with STGD1 (F = 16.7; $P = 0.0003$) but not those of the fast rod ERG signals (F = 3.6; $P = 0.07$). The ERG phases of neither the slow pathway (F = 1.3; $P = 0.30$) nor the fast pathway (F = 1.2; $P = 0.36$) were significantly influenced by the clinical parameters: age, age-adjusted disease duration, visual acuity, and the distribution of flecks. Similarly to the amplitude data, the intraindividual interocular differences were considerably low (median for the slow rod ERG signals between 6° and 13°; for the fast rod ERG signals between 4° and 9°). Probabilities for testing the hypothesis that eyes with better visual acuity exhibited larger ERG response phases (corresponding to shorter implicit times) ranged between 0.04 and 0.64 for the slow rod ERG signals and between 0.09 and 0.66 for the fast rod ERG signals, but a subsequent Bonferroni-Holm adjustment to correct for multiple comparisons (multiple $\alpha = 0.05$) revealed that none of these measures was significant.

Standard Scotopic ERG

A summary of all standard ERG measures of individual patients with STGD1 is given in Table 2. The amplitudes of the scotopic rod b-wave, the scotopic a-wave, and the b-wave of the maximal response were below the normal 5th percentile in 22, 14, and 15, of 54 eyes, respectively (Table 2). The implicit times of the scotopic rod b-wave, and the a- and the b-wave of the maximal response were above the 95th percentile in the normal subjects in 15, 12, and 22 of 54 eyes, respectively (Table 2).

The amplitudes and implicit times of the standard scotopic ERG were statistically analyzed with an ANOVA. For the scotopic rod b-wave amplitude to a dim white flash, the ANOVA revealed a lower mean in the STGD1 group ($t = 2.5$; $P = 0.02$), but there was no difference in implicit time ($t = -0.71$; $P = 0.48$). The scotopic a-wave was lower in amplitude ($t = 2.3$; $P = 0.03$) and prolonged in implicit time ($t = 2.6$; $P = 0.01$). For the scotopic b-wave to the maximal flash, there was no difference in amplitude ($t = 2.0$; $P = 0.06$), but the implicit time was prolonged in the patients with STGD1 ($t = -2.5$; $P = 0.02$). The b- to a-wave ratio did not show a difference ($t = -0.58$; $P = 0.56$). A subsequent Bonferroni-Holm adjustment to correct for multiple comparisons (multiple $\alpha = 0.05$), however, revealed that none of these measures exhibited significant differences between subject groups.

We also examined the canonical correlation of the amplitudes and phases of both the slow and fast rod ERG signals with the respective measures derived from the standard ERG (Table 3). Generally, the amplitude data were highly correlated, whereas there were only weak or moderate correlations between ERG phases and ERG implicit times. Subsequent Bonferroni-Holm adjustments (multiple $\alpha = 0.05$) revealed that all correlations between the amplitude data were significant, whereas only the phases of the slow rod ERG signals and the a-wave implicit time were significantly correlated, and all other correlations between phase data and implicit times were not.

DISCUSSION

In a group of 27 patients with STGD1 who had mutations in both alleles for the *ABCA4* gene we found significantly decreased amplitudes for both the slow and fast rod signals

TABLE 2. Scotopic Standard ERG of the Patients with STGD1

	Rod Response b-Wave				a-Wave				Maximum Response: b-Wave					
	Amplitude		Implicit time		Amplitude		Implicit time		Amplitude		Implicit time		b- to a-Wave Ratio	
Patient	OD	OS	OD	OS	OD	OS	OD	OS	OD	OS	OD	OS	OD	OS
1	95.1	117.7	96.5	97.5	73.2	84.8	19.0	19.5	185.4	261.6	56.5	58.5	2.53	3.09
2	175.6	181.7	104.5	105.5	205.5	186.6	21.5	21.0	371.3	351.8	51.0	51.0	1.81	1.89
3	232.3	238.4	96.5	95.5	282.9	253.7	21.0	21.0	442.1	397.6	45.5	46.0	1.56	1.57
4	195.1	176.2	104.0	105.5	156.7	135.4	22.0	22.5	369.5	317.7	47.5	47.5	2.36	2.35
5	170.1	226.2	110.5	111.0	174.4	189.0	22.0	22.5	462.2	536.0	49.0	49.0	2.65	2.84
6	185.4	151.2	106.5	103.5	143.3	172.6	21.5	21.5	419.5	398.2	47.0	46.5	2.93	2.31
7	364.6	536.6	92.5	103.0	205.5	241.5	21.5	17.0	482.3	611.6	48.0	49.5	2.35	2.53
8	197.0	103.7	111.5	112.5	189.6	120.7	23.0	23.5	298.2	204.3	50.5	48.0	1.57	1.69
9	181.1	207.3	70.5	78.5	254.3	262.2	21.5	20.5	558.5	559.8	43.0	46.5	2.20	2.13
10	242.7	182.3	74.5	77.0	216.5	218.3	16.5	15.5	372.0	403.1	46.0	46.5	1.72	1.85
11	254.3	234.2	105.5	105.0	207.9	192.7	20.5	20.5	498.2	464.0	41.0	40.0	2.40	2.41
12	163.4	134.8	68.5	74.5	174.4	173.2	19.5	20.5	273.2	320.1	33.0	34.0	1.57	1.85
13	207.3	156.1	107.0	109.0	237.8	168.3	21.5	21.0	429.9	287.8	45.0	44.5	1.81	1.71
14	28.1	14.6	109.0	90.5	37.2	62.8	24.0	25.5	82.3	92.1	56.0	58.5	2.21	1.47
15	272.0	242.7	90.5	90.5	214.0	164.0	16.0	21.0	406.1	333.5	36.5	36.0	1.90	2.03
16	13.4	23.8	115.5	115.0	26.2	35.4	23.5	25.5	37.2	68.3	55.5	56.5	1.42	1.93
17	214.0	265.2	87.0	89.5	262.8	288.4	21.5	21.5	373.2	467.7	35.0	35.0	1.42	1.62
18	76.2	59.2	93.5	93.0	144.5	187.8	23.0	24.0	203.7	164.0	43.0	44.5	1.41	0.87
19	87.2	62.8	110.5	108.5	97.6	75.6	22.5	23.5	178.7	120.1	45.0	44.5	1.83	1.59
20	295.7	323.2	79.5	79.5	206.1	215.2	21.0	21.5	442.7	501.8	47.0	47.0	2.15	2.33
21	322.6	266.5	95.5	96.0	264.0	198.2	19.0	17.0	464.6	396.3	45.0	44.0	1.76	2.00
22	328.7	262.2	71.5	97.0	341.5	194.5	15.5	15.5	594.5	338.4	43.0	43.0	1.74	1.74
23	239.0	270.1	88.0	89.5	169.5	198.8	21.0	21.0	297.6	351.8	34.5	35.0	1.76	1.77
24	389.6	383.5	77.5	78.5	307.3	309.2	20.0	20.0	680.5	662.2	47.0	46.5	2.21	2.14
25	181.7	265.2	72.0	86.5	192.7	223.2	15.5	15.5	331.1	407.9	47.5	49.0	1.72	1.83
26	415.9	261.6	96.0	98.5	337.2	205.5	21.5	22.0	743.9	468.9	54.0	50.5	2.21	2.28
27	269.3	259.2	96.5	95.5	186.6	251.2	22.0	21.5	436.0	407.9	47.5	48.0	2.34	1.62
Median	**212.5**		**96.0**		**200.3**		**21.3**		**387.5**		**46.8**		**1.85**	
5th perc	35.2		74.9		58.7		15.5		105.9		34.8		1.53	
95th perc	372.2		111.6		274.3		24.0		592.2		56.9		2.71	
Normal Median	**268.3**		**91.0**		**222.6**		**20.5**		**438.4**		**43.3**		**1.89**	
Normal 5th perc	184.2		84.5		168.3		15.0		317.7		33.0		1.55	
Normal 95th perc	435.4		105.0		282.9		22.0		537.2		47.0		2.39	

Results of the ERG recordings according to the ISCEV standard of the individual patients. Scotopic rod b-wave amplitude (in microvolts) and implicit time (in milliseconds), a-wave amplitude of the maximal response (in microvolts), and implicit time (in milliseconds), b-wave amplitude (in microvolts), and implicit time (in milliseconds) of the maximum response, and the b- to a-wave ratio are shown for the right and left eyes. For the scotopic standard ERG, the lower lines provide the median and the 5th and 95th percentiles of the patients (two-eye medians) and of the normal subjects.

derived from the scotopic 15-Hz flicker ERG. The ERG response phase of the slow rod signals lagged significantly. The amplitude data exhibited significant correlation between the scotopic 15-Hz flicker ERG and the standard rod ERG, whereas this was not generally the case for the ERG timing. The abnormalities of the standard rod ERG measures themselves did not reach statistical significance, although 41% of the eyes tested exhibited subnormal rod b-wave amplitudes.

In previous studies involving the scotopic standard ERG, investigators have reported equivocal results. Moreover, in these studies patients were not genotyped. In one study, highly significant amplitude losses were reported in STGD1,[23] whereas in another study all patients showed completely normal scotopic ERGs.[21] In other studies, only a minority of patients with STGD1 exhibited reduced scotopic rod b-waves,[13,20,22,24–26,40] which is in accordance with our findings. It is known that STGD1 exhibits a large interindividual variability in clinical severity (e.g., Refs. 19,41), which is also true for our group of patients with STGD1. This may explain why our patients with STGD1 as a group did not show a statistically significant reduction in ERG amplitude or an increase in implicit time. In the majority of previous studies, however, the timing of the scotopic rod b-wave has not been investigated. In a few studies, either mildly or rarely abnormal implicit times were reported,[24] which is in accordance with our results, whereas in another complete normality was reported.[21] We conclude that standard ERG techniques may fail to detect subtle deterioration within the rod system in STGD1.

Anatomic and physiological studies of the mammalian retina have revealed the existence of separate rod pathways. Rods are thought to synapse with a single type of bipolar cell, the rod ON bipolar cell.[42–44] This cell, in turn, contacts the AII amacrine cell at a sign-preserving glutamate synapse.[45–49] Signals from the AII cell then infiltrate the main cone circuitry by exciting ON cone bipolar cells and inhibiting OFF cone bipolar cells.[46,49–51] Thereafter, ON bipolar cells excite ON ganglion cells, and OFF bipolar cells excite OFF ganglion cells. A second pathway (the rod–cone coupling pathway) infiltrates the ON and OFF cone bipolar circuitry at the earliest possible stage, through gap junction contacts between rod and cone photoreceptors, facilitating electrical transmission.[47,52–54] Through these gap junctions, signal flow involves ON and OFF cone bipolar cells and thereafter ON and OFF ganglion cells.[47,53,55,56] There is plenty of evidence from electrophysiological and psychophysical studies by Stockman et al.[28,29] and

TABLE 3. Canonical Correlation between the Slow and Fast Rod ERG Signals and the Standard ERG Parameters

	Rod Response b-Wave		Maximum Response a-Wave		Maximum Response b-Wave	
	Amplitude	**Implicit Time**	**Amplitude**	**Implicit Time**	**Amplitude**	**Implicit Time**
ERG amplitudes: slow rod ERG pathway						
r	0.70		0.63		0.63	
P	<0.0001	—	<0.0001	—	<0.0001	—
n	54		54		54	
ERG amplitudes: fast rod ERG pathway						
r	0.62		0.50		0.52	
P	<0.0001	—	<0.0001	—	<0.0001	—
n	54		54		54	
ERG phases: slow rod ERG pathway						
r		0.19		0.44		0.37
P	—	0.36	—	0.002	—	0.06
n		26		46		26
ERG phases: fast rod ERG pathway						
r		0.27		0.32		0.37
P	—	0.15	—	0.02	—	0.04
n		31		50		31

Canonical correlations of the amplitudes and phases of both the slow and fast rod ERG signals with the respective measures derived from the standard ERG. The data provide the canonical correlation coefficient (*r*), the probability (*P*, not corrected for multiple comparisons), and the sample size (*n*).

Sharpe and Stockman[30] that the slow and fast rod ERG signals revealed in the human scotopic 15-Hz flicker ERG reflect electrophysiological activity driven by the rod bipolar–AII cell pathway and the rod–cone coupling pathway, respectively.[28–30] In preliminary observations in two patients with congenital stationary night blindness of the complete Schubert-Bornschein type, Sharpe and Stockman[30] could not find detectable fast rod ERG signals, which is inconsistent with their model of a rod–cone coupling pathway. In a very recent study in patients with CSNB1 who carried mutations in the *NXY* gene, however, we could detect substantial fast rod ERG signals,[39] which provides further support for the model suggested by Stockman et al.,[28,29] Sharpe and Stockman,[30] and Sharpe et al.[57,58]

It cannot be ruled out, however, that a direct rod-to-cone OFF bipolar cell pathway that has been recently described in the wild-type mouse[59] may be involved in generating the scotopic 15-Hz flicker ERG. To date, however, it is unclear whether this third rod pathway is common to all mammalian retinas.[60] It has been hypothesized[29] that the scotopic 15-Hz flicker ERG reflects electrical activity, mainly of rod and cone bipolar cells, although many retinal elements (such as the receptors, the rod–cone gap junctions, or the AII cells) could be involved.

We provide evidence that in STGD1 both rod pathways can be functionally affected. The scotopic 15-Hz flicker ERG may reveal subtle abnormalities at different sites within the rod system that remain undetected by standard ERG techniques. Nevertheless, why the scotopic 15-Hz flicker ERG revealed abnormalities for both the slow and fast rod ERG signals in the patients as a group, whereas the standard ERG did not show significant effects, remains speculative. The comparison, however, is complicated, because the single-flash ERG and the scotopic 15-Hz flicker ERG are measured under very different conditions: The single-flash ERG is measured with flashes that are separated in time with the express purpose of avoiding the effects of light adaptation, whereas the scotopic 15-Hz flicker ERG is measured with prolonged trains of flashes. As a result, light adaptation plays a much greater role in the production of the scotopic 15-Hz flicker ERG than of the single-flash ERG response.[28] Moreover, the slow rod signals are obtained by applying stimuli that are considerably less intense than the dim white flash used to obtain the standard rod response.[32] (The standard rod b-wave is measured with flash intensities at which we obtained the fast rod signals—i.e., −0.97 log scot td · sec; cf. Figs. 1, 2, 3.) Therefore, it may be that alteration within the slow rod ERG pathway generally cannot be detected by the standard rod ERG. These considerations are specifically important when comparing the measures of the two different ERG techniques and may explain why there is only mild correlation for the timing (Table 3).

Correlation of electrophysiological measures with clinical parameters such as the fundus appearance was observed by some investigators,[13,19,25] whereas others denied such a correlation.[21] In accordance with the former, the amplitude loss for both the slow and fast rod signals were highly correlated with the combination of the clinical parameters: age, age-adjusted disease duration, visual acuity, and the distribution of flecks. However, apart from the significant correlation of visual acuity and amplitude of the slow rod signals, no parameter alone exhibited a significant correlation. We suggest that the parameters such as visual acuity, disease duration, and fundus flecks taken together reflect the severity of STGD1. Thus, the severity of the disease very well influences the functional outcome reflected in the scotopic 15-Hz flicker ERG. We conclude that all single parameters have to be considered in connection, to evaluate disease severity, even though visual acuity alone is a very important measure.

Mutational analysis of the *ABCA4* gene revealed missense, nonsense, frameshift, and splice mutations in our study group. Although the majority of patients were shown to carry two missense (mild-moderate mutation) or one missense and one protein truncating mutation (severe mutation), five probands all share the splice mutation 2588G→C on one allele and, in addition, have a protein-truncating mutation (nonsense or splice mutation) on the second. The 2588G→C transversion is a relatively common mutation but is also present in control individuals with a surprisingly high allele frequency.[7,10] It has

been calculated that the predicted homozygote frequency for this allele alone is greater than the estimated 1 in 10,000 incidence of STGD1.[7] Taking this into account, as well as the observed scarcity of 2588G→C homozygotes, Maugeri et al.[7] suggested that 2588G→C may be a mild mutation, only causing disease when in combination with a severe allele. A recent functional study has supported this view and shown that the two products of the 2588G→C mutation, G863A and delG863, produce a substantially impaired and a mildly impaired protein, respectively.[61] Genetically, our STGD1 study group therefore appears to be relatively uniform, in the sense that in none of the patients there were two protein-truncating disease alleles. This and the fact that the number of patients with a certain combination of disease alleles was too small does not make any specific correlation between mutation-combination of mutation and clinical phenotype meaningful.

Within the photoreceptor outer segments, ABCA4 localizes to the disc rather than the plasma membrane, and within the disc membrane it is confined to the rim.[3,62] This localization strongly suggests that ABCA4 catalyzes the intracellular rather than intercellular transport of a substrate. The recently described phenotype of *ABCA4* knockout mice strongly supports a role for the ABCA4 transporter in intraphotoreceptor retinoid transport. The targeted mice show more all-*trans* retinal and less all-*trans* retinol in the retina after acute light exposure, and, over time, they accumulate A2-E in the RPE, presumably because of the build-up of all-*trans* retinal within the photoreceptor disc membranes.[18] These data suggest that ABCA4 normally transports or extracts all-*trans* retinal from the disc membranes (after its release from photoactivated rhodopsin), presenting it as a substrate for all-*trans* retinal dehydrogenase, the enzyme within the outer segment that converts all-*trans* retinal to all-*trans* retinol before its export and subsequent reisomerization in the RPE.[63] It has been proposed that ABCA4-mediated photoreceptor death finally results from loss of the RPE support function.[18] Accordingly, the a-wave is normal in young *ABCA4* knockout mice, but abnormal in older animals. This suggests that the ERG amplitude reductions (for both the slow and fast rod ERG pathways) we found in patients with STGD1 result from secondary photoreceptor effects mediated by the loss of the RPE support function. This mechanism at the RPE-photoreceptor level renders unexplained the differently affected timing of the rod ERG signals we found in our patients.

However, one should be cautious about directly deducing the morphologic and functional consequences for the human disease from the *ABCA4* knockout mouse model. In a human retina with longstanding fundus flavimaculatus, histologic study indicated, apart from shortened outer segments and photoreceptor loss, reactive Müller cell hypertrophy, and accumulation of lipofuscin in the photoreceptor inner segments peripheral to the macular area. This latter observation derived from a rod-dominated fundus region may serve as an explanation of the phase lag (time delay) we observed in the slow rod pathway of our patients, if we assume that the rod–cone gap junctions and the cone inner segments remain relatively intact. Accumulation of metabolites in the rod inner segments may well impair the signal flow to rod ON bipolar cells in the slow rod pathway. Similar observations have been made in retinitis pigmentosa, an inherited rod photoreceptor dystrophy. Some patients with this disease (e.g., patients with a rhodopsin intron 4 splice-site mutation) show disproportional postreceptoral function loss in the ERG that cannot be explained by photoreceptor outer segment loss alone.[64,65] Histologic studies in mice expressing the rhodopsin Q344ter transgene have revealed abnormal accumulation of the mutant gene product in the inner segment,[66] which, in addition to outer segment dysfunction, may impair synaptic transmission of the rod outer segment signal. In a single patient with the rhodopsin Q344ter mutation, we have observed abnormal timing only in the slow rod ERG signals derived from the scotopic 15-Hz flicker ERG,[27] which suggests damage not only at the level of the outer segments but also at or proximal to the photoreceptor terminal region. It is tempting to speculate whether the phase lag we observed only in the slow rod ERG signals of patients with STGD1 reflects a similar disease mechanism.

Acknowledgments

The authors thank Kathrin Vohrer for technical assistance and Eberhart Zrenner for general support.

References

1. Papermaster DS, Schneider BG, Zorn MA, Kraehenbuhl JP. Immunocytochemical localization of a large intrinsic membrane protein to the incisures and margins of frog rod outer segment disks. *J Cell Biol.* 1978;78:415–425.
2. Azarian SM, Travis GH. The photoreceptor rim protein is an ABC transporter encoded by the gene for recessive Stargardt's disease (ABCR). *FEBS Lett.* 1997;409:247–252.
3. Illing M, Molday LL, Molday RS. The 220-kDa rim protein of retinal rod outer segments is a member of the ABC transporter superfamily. *J Biol Chem.* 1997;272:10303–10310.
4. Thomson JL, Brzeski H, Dunbar B, et al. Photoreceptor rim protein: partial sequences of cDNA show a high degree of similarity to ABC transporters. *Curr Eye Res.* 1997;16:741–745.
5. Allikmets R, Singh N, Sun H, et al. A photoreceptor cell-specific ATP-binding transporter gene (ABCR) is mutated in recessive Stargardt macular dystrophy. *Nat Genet.* 1997;15:236–246.
6. Lewis RA, Shroyer NF, Singh N, et al. Genotype/phenotype analysis of a photoreceptor-specific ATP-binding cassette transporter gene, ABCR, in Stargardt disease. *Am J Hum Genet.* 1999;64:422–434.
7. Maugeri A, van Driel MA, van de Pol DJ, et al. The 2588G→C mutation in the ABCR gene is a mild frequent founder mutation in the Western European population and allows the classification of ABCR mutations in patients with Stargardt disease. *Am J Hum Genet.* 1999;64:1024–1035.
8. Nasonkin I, Illing M, Koehler MR, et al. Mapping of the rod photoreceptor ABC transporter (ABCR) to 1p21–p22.1 and identification of novel mutations in Stargardt's disease. *Hum Genet.* 1998;102:21–26.
9. Rozet JM, Gerber S, Souied E, et al. Spectrum of ABCR gene mutations in autosomal recessive macular dystrophies. *Eur J Hum Genet.* 1998;6:291–295.
10. Rivera A, White K, Stohr H, et al. A comprehensive survey of sequence variation in the ABCA4 (ABCR) gene in Stargardt disease and age-related macular degeneration. *Am J Hum Genet.* 2000;67:800–813.
11. Stargardt K. Über familiäre, progressive Degenerationen im Kindesalter. *Graefes Arch Clin Exp Ophthalmol.* 1909;71:534–550.
12. Franceschetti A. Über tapeto-retinale Degenerationen im Kindesalter. In: Sautter H, ed. *Entwicklung und Fortschritt in der Augenheilkunde.* Stuttgart: Enke; 1963:107–120.
13. Armstrong JD, Meyer D, Xu S, Elfervig JL. Long-term follow-up of Stargardt's disease and fundus flavimaculatus. *Ophthalmology.* 1998;105:448–457.
14. Anderson KL, Baird L, Lewis RA, et al. A YAC contig encompassing the recessive Stargardt disease gene (STGD) on chromosome 1p. *Am J Hum Genet.* 1995;57:1351–1363.
15. Krill AE, Deutman AF. The various categories of juvenile macular degeneration. *Trans Am Ophthalmol Soc.* 1972;70:220–245.
16. Molday LL, Rabin AR, Molday RS. ABCR expression in foveal cone photoreceptors and its role in Stargardt macular dystrophy. *Nat Genet.* 2000;25:257–258.
17. Scholl HPN, Kremers J, Vonthein R, White K, Weber BH. L- and M-cone driven electroretinograms in Stargardt's macular dystrophy-fundus flavimaculatus. *Invest Ophthalmol Vis Sci.* 2001;42:1380–1389.
18. Weng J, Mata NL, Azarian SM, et al. Insights into the function of Rim protein in photoreceptors and etiology of Stargardt's disease from the phenotype in abcr knockout mice. *Cell.* 1999;98:13–23.

19. Fishman GA. Fundus flavimaculatus: a clinical classification. *Arch Ophthalmol.* 1976;94:2061–2067.
20. Hadden OB, Gass JD. Fundus flavimaculatus and Stargardt's disease. *Am J Ophthalmol.* 1976;82:527–539.
21. Noble KG, Carr RE. Stargardt's disease and fundus flavimaculatus. *Arch Ophthalmol.* 1979;97:1281–1285.
22. Niemeyer G, Demant E. Cone and rod ERGs in degenerations of central retina. *Graefes Arch Clin Exp Ophthalmol.* 1983;220:201–208.
23. Moloney JB, Mooney DJ, O'Connor MA. Retinal function in Stargardt's disease and fundus flavimaculatus. *Am J Ophthalmol.* 1983; 96:57–65.
24. Lachapelle P, Little JM, Roy MS. The electroretinogram in Stargardt's disease and fundus flavimaculatus. *Doc Ophthalmol.* 1989; 73:395–404.
25. Stavrou P, Good PA, Misson GP, Kritzinger EE. Electrophysiological findings in Stargardt's-fundus flavimaculatus disease. *Eye.* 1998; 12:953–958.
26. Lois N, Holder GE, Fitzke FW, Plant C, Bird AC. Intrafamilial variation of phenotype in Stargardt macular dystrophy-fundus flavimaculatus. *Invest Ophthalmol Vis Sci.* 1999;40:2668–2675.
27. Scholl HPN, Langrová H, Weber BH, Zrenner E, Apfelstedt-Sylla E. Clinical electrophysiology of two rod pathways: normative values and clinical application. *Graefes Arch Clin Exp Ophthalmol.* 2001; 239:71–80.
28. Stockman A, Sharpe LT, Rüther K, Nordby K. Two signals in the human rod visual system: a model based on electrophysiological data. *Vis Neurosci.* 1995;12:951–970.
29. Stockman A, Sharpe LT, Zrenner E, Nordby K. Slow and fast pathways in the human rod visual system: electrophysiology and psychophysics. *J Opt Soc Am A.* 1991;8:1657–1665.
30. Sharpe LT, Stockman A. Rod pathways: the importance of seeing nothing. *Trends Neurosci.* 1999;22:497–504.
31. Birnbach CD, Jarvelainen M, Possin DE, Milam AH. Histopathology and immunocytochemistry of the neurosensory retina in fundus flavimaculatus. *Ophthalmology.* 1994;101:1211–1219.
32. Marmor MF, Zrenner E. Standard for clinical electroretinography (1999 update): International Society for Clinical Electrophysiology of Vision. *Doc Ophthalmol.* 1998;97:143–156.
33. Wyszecki G, Stiles W. *Color Science: Concepts and Methods, Quantitative Data and Formulas.* New York: John Wiley & Sons; 1982.
34. Birch DG, Fish GE. Rod ERGs in retinitis pigmentosa and cone-rod degeneration. *Invest Ophthalmol Vis Sci.* 1987;28:140–150.
35. Usui T, Kremers J, Sharpe LT, Zrenner E. Flicker cone electroretinogram in dichromats and trichromats. *Vision Res.* 1998;38:3391–3396.
36. Harris CM. The Fourier analysis of biological transients. *J Neurosci Methods.* 1998;83:15–34.
37. Muthuswamy J, Thakor NV. Spectral analysis methods for neurological signals. *J Neurosci Methods.* 1998;83:1–14.
38. Ray WA, O'Day DM. Statistical analysis of multi-eye data in ophthalmic research. *Invest Ophthalmol Vis Sci.* 1985;26:1186–1188.
39. Scholl HPN, Langrová H, Pusch CM, et al. Slow and fast rod ERG pathways in patients with X-linked complete stationary night blindness carrying mutations in the *NYX* gene. *Invest Ophthalmol Vis Sci.* 2001;42:2728–2736.
40. Itabashi R, Katsumi O, Mehta MC, et al. Stargardt's disease/fundus flavimaculatus: psychophysical and electrophysiologic results. *Graefes Arch Clin Exp Ophthalmol.* 1993;231:555–562.
41. Fishman GA, Stone EM, Grover S, et al. Variation of clinical expression in patients with Stargardt dystrophy and sequence variations in the ABCR gene. *Arch Ophthalmol.* 1999;117:504–510.
42. Boycott BB, Dowling JE. Organization of the primate retina: Light microscopy. *Philos Trans R Soc Lond B.* 1969;255:109–184.
43. Dacheux RF, Raviola E. The rod pathway in the rabbit retina: a depolarizing bipolar and amacrine cell. *J Neurosci.* 1986;6:331–345.
44. Wässle H, Boycott BB. Functional architecture of the mammalian retina. *Physiol Rev.* 1991;71:447–480.
45. Chun MH, Han SH, Chung JW, Wässle H. Electron microscopic analysis of the rod pathway of the cat retina. *J Comp Neurol.* 1993;332:421–432.
46. Kolb H, Famiglietti EV. Rod and cone pathways in the inner plexiform layer of the cat retina. *Science.* 1974;186:47–49.
47. Kolb H, Nelson R. Rod pathways in the retina of the cat. *Vision Res.* 1983;23:301–312.
48. McGuire BA, Stevens JK, Sterling P. Microcircuitry of bipolar cells in cat retina. *J Neurosci.* 1984;4:2920–2938.
49. Wässle H, Grunert U, Chun MH, Boycott BB. The rod pathway of the macaque monkey retina: identification of AII-amacrine cells with antibodies against calretinin. *J Comp Neurol.* 1995;361:537–551.
50. Famiglietti EV, Kolb H. A bistratified amacrine cell and synaptic circuitry in the inner plexiform layer of the retina. *Brain Res.* 1975;84:293–300.
51. Müller F, Wässle H, Voigt T. Pharmacological modulation of the rod pathway in the cat retina. *J Neurophysiol.* 1988;59:1657–1672.
52. Kolb H. The organization of the outer plexiform layer in the retina of the cat: electron microscopy observations. *J Neurocytol.* 1977; 6:131–153.
53. Nelson R. Cat cones have rod input: a comparison of the response properties of cone-horizontal cell bodies in the retina of the cat. *J Comp Neurol.* 1977;172:109–136.
54. Raviola E, Gilula NB. Intramembrane organization of specialized contacts in the outer plexiform layer of the retina. *J Cell Biol.* 1975;65:192–222.
55. Smith RG, Freed MA, Sterling P. Microcircuitry of the dark-adapted cat retina: functional architecture of the rod-cone network. *J Neurosci.* 1986;6:3505–3517.
56. Sterling P, Freed MA, Smith RG. Microcircuitry and functional architecture of the cat retina. *Trends Neurosci.* 1986;9:186–192.
57. Sharpe LT, Stockman A, Macleod DI. Rod flicker perception: scotopic duality, phase lags and destructive interference. *Vision Res.* 1989;29:1539–1559.
58. Sharpe LT, Fach CC, Stockman A. The spectral properties of the two rod pathways. *Vision Res.* 1993;33:2705–2720.
59. Hack I, Peichl L, Brandstätter JH. An alternative pathway for rod signals in the rodent retina: rod photoreceptors, cone bipolar cells, and the localization of glutamate receptors. *Proc Natl Acad Sci USA.* 1999;96:14130–14135.
60. Bloomfield SA, Dacheux RF. Rod vision: pathways and processing in the mammalian retina. *Prog Retinal Eye Res.* 2001;20:351–384.
61. Sun H, Smallwood PM, Nathans J. Biochemical defects in ABCR protein variants associated with human retinopathies. *Nat Genet.* 2000;26:242–246.
62. Sun H, Nathans J. Stargardt's ABCR is localized to the disc membrane of retinal rod outer segments. *Nat Genet.* 1997;17:15–16.
63. Rattner A, Sun H, Nathans J. Molecular genetics of human retinal disease. *Annu Rev Genet.* 1999;33:89–131.
64. Cideciyan AV, Jacobson SG. Negative electroretinograms in retinitis pigmentosa. *Invest Ophthalmol Vis Sci.* 1993;34:3253–3263.
65. Jacobson SG, Kemp CM, Cideciyan AV, et al. Phenotypes of stop codon and splice site rhodopsin mutations causing retinitis pigmentosa. *Invest Ophthalmol Vis Sci.* 1994;35:2521–2534.
66. Sung CH, Makino C, Baylor D, Nathans J. A rhodopsin gene mutation responsible for autosomal dominant retinitis pigmentosa results in a protein that is defective in localization to the photoreceptor outer segment. *J Neurosci.* 1994;14:5818–5833.